

Structural and electronic properties of hydrogen adsorptions on BC_3 sheet and graphene: a comparative study

This article has been downloaded from IOPscience. Please scroll down to see the full text article.

2011 Nanotechnology 22 135703

(<http://iopscience.iop.org/0957-4484/22/13/135703>)

View [the table of contents for this issue](#), or go to the [journal homepage](#) for more

Download details:

IP Address: 163.28.112.100

The article was downloaded on 14/09/2011 at 02:57

Please note that [terms and conditions apply](#).

Structural and electronic properties of hydrogen adsorptions on BC₃ sheet and graphene: a comparative study

Feng-Chuan Chuang¹, Zhi-Quan Huang¹, Wen-Huan Lin¹,
Marvin A Albao^{1,3} and Wan-Sheng Su^{2,4}

¹ Department of Physics, National Sun Yat-sen University, Kaohsiung 804, Taiwan

² National Center for High-Performance Computing, Tainan 741, Taiwan

E-mail: wssu@nchc.narl.org.tw

Received 29 November 2010, in final form 31 January 2011

Published 22 February 2011

Online at stacks.iop.org/Nano/22/135703

Abstract

We have systematically investigated the effect of hydrogen adsorption on a single BC₃ sheet as well as graphene using first-principles calculations. Specifically, a comparative study of the energetically favorable atomic configurations for both H-adsorbed BC₃ sheets and graphene at different hydrogen concentrations ranging from 1/32 to 4/32 ML and 1/8 to 1 ML was undertaken. The preferred hydrogen arrangement on the single BC₃ sheet and graphene was found to have the same property as that of the adsorbed H atoms on the neighboring C atoms on the opposite sides of the sheet. Moreover, at low coverage of H, the pattern of hydrogen adsorption on the BC₃ shows a proclivity toward formation on the same ring, contrasting their behavior on graphene where they tend to form the elongated zigzag chains instead. Lastly, both the hydrogenated BC₃ sheet and graphene exhibit alternation of semiconducting and metallic properties as the H concentration is increased. These results suggest the possibility of manipulating the bandgaps in a single BC₃ sheet and graphene by controlling the H concentrations on the BC₃ sheet and graphene.

(Some figures in this article are in colour only in the electronic version)

1. Introduction

Spurred by the creation of graphene in the laboratory recently, two-dimensional graphene has sparked interest among theoretical and experimental researchers due to its characteristic electronic properties. It is well established that a pristine layer of graphene is a zero-gap semiconductor with a point-like Fermi surface and a linear dispersion at the Fermi level near the K-point. Typically, it is possible to tailor the desired bandgap for such a system via formation of nanoribbons by cutting a graphene sheet [1, 2] or by attaching foreign atoms to the pristine layer [3–5]. It was Son *et al* [6] who demonstrated that H-terminated graphene nanoribbons with either armchair- or zigzag-shaped edges have

a nonzero energy gap, a finding later confirmed by Li *et al* [7] and Ritter *et al* [8]. Son *et al* [9] likewise predicted that the zigzag graphene nanoribbons are half-metallic in the presence of an external electric field. Coincidentally, numerous parallel studies on the modified graphene surfaces have been reported, and the resulting electronic properties are shown to be similar to that of pure graphene, albeit altered by the presence of foreign atoms attached. For instance, Ryu *et al* [10] showed that graphene can chemically react with hydrogen and further showed that this hydrogenation is reversible. Likewise, Elias *et al* [11] demonstrated that graphene can chemically react with hydrogen to form an insulating derivative called graphane. Collectively, these discoveries point toward interesting underlying physics and hint at potential applications in the emerging field of nanoelectronics such as spin-dependent switching devices and hydrogen storage.

³ Present address: National Energy Technology Laboratory, US Department of Energy, Pittsburgh, PA 15236, USA.

⁴ Author to whom any correspondence should be addressed.

Boron atoms have been widely used as dopants in carbon nanostructures for building functional materials owing to their similar atomic radius. Not surprisingly, a uniform BC_3 sheet has already been synthesized in the laboratory [12, 13]. Its geometric structure was found to be almost identical to graphene, except that some carbon atoms are replaced by boron atoms so that six carbon atoms form a hexagon surrounded by six boron atoms [14, 15]. In addition, Pontes *et al* found that boron atoms can substitute carbon atoms in a graphene sheet without any activation barrier [16]. However, it should be stressed that the BC_3 honeycomb sheet is a semiconductor with an indirect gap, while graphene is a semiconductor with a zero gap. Recent theoretical works [14, 15, 17, 18] revealed that the tunable electronic properties of the BC_3 sheet are feasible. Similar to the graphene nanoribbon [7], the BC_3 sheets can be cut into BC_3 nanoribbons. As such, armchair edge BC_3 nanoribbons are semiconducting, whereas zigzag edge BC_3 nanoribbons are either semiconducting or metallic, depending on the edge atoms [17]. Moreover, the study by Ding *et al* [18] further indicated that hydrogen adsorption in BC_3 sheets results in the appearance of a semiconductor–semiconductor–metal transition. Thus, following graphene, the BC_3 sheet should be a good candidate for potential applications.

Based on the preceding discussions, a potentially novel idea on hydrogen storage emerges—the capture of molecular hydrogen with carbon-based materials. In addition to the previously proposed elongated carbon nanotubes, the two-dimensional sheet materials constitute another viable choice for hydrogen storage. For the fully hydrogenated graphene, conformations in which each carbon atom alternately bonded with a hydrogen atom on either side of the plane is shown to be the most stable [4, 19]. Likewise, at certain coverages, the hydrogenation of the BC_3 sheet behaves similarly as graphene [18]. The results revealed that, at certain low coverages of H, graphene is semiconducting, whereas the fully hydrogenated BC_3 has metallic properties [18]. In contrast, in the case of the hydrogenation of graphene the reverse is true, i.e. it exhibits semiconducting characteristics at high coverages and metallic properties at low coverages. All of these intriguing findings suggest that, despite the preponderance of previous experimental and theoretical efforts on the topic, a thorough and definitive inquiry into the hydrogenation process of both graphene and BC_3 sheets is in order. Hence, we embark on a systematic method to determine the atomic structures of hydrogenation of such sheets at different H coverages. In this work, a comparative study of the H adsorptions on graphene and the single BC_3 sheet will be the focus.

In the present study, a systematic search based on a combinatorial method for uncovering optimized atomic structures of hydrogen-adsorbed graphene and a BC_3 sheet was employed. Likewise, the electronic properties of our identified structures were analyzed in detail. The rest of the paper is organized as follows: in section 2, we describe our computational methods and procedures. In section 3, we present structural models from our search and subsequently analyze them in detail. Finally, we summarize our major findings with a brief conclusion in section 4.

2. Computational methods

2.1. Tree structure

To understand the hydrogenation process of BC_3 and graphene, we performed a combinatorial search for all the possible adsorptions on a single sheet based on a tree structure. In our search, we first used the 2×2 supercell containing eight atoms. We further assumed the H atoms were adsorbed on the lowest energy atomic structure of the BC_3 sheet that was previously identified by Wang *et al* [15]. One monolayer of H coverage is defined as having one H atom adsorbed on each atom on the sheet. Furthermore, these hydrogen atoms could be adsorbed on either side of the sheet as shown in figure 1(a). It follows that, for the 2×2 supercell, there are totally 16 possible adsorption sites. The supercell can be represented either as a hexagon (dashed lines) or a parallelogram (solid lines) as seen in figure 1(b). If a hydrogen atom was already adsorbed on the atom on one side of the sheet, the corresponding site on the other side belonging to the same atom is deemed forbidden (i.e. not available for adsorption). Based on these considerations, the total number of possible configurations for n hydrogen atoms adsorbed on the sheet is $C_n^8 \times 2^n$ ($n = 1-8$).

Next, using the tree structure [20] as the data structure to generate and store all the possible structures, we first index the hydrogen adsorption site, p , from 1 through N , where N is the number of sites in the supercell. For the 2×2 supercell, the number of possible absorptions, N , is 16. Additionally, a sequence for placing atoms is defined such that each level in the tree structure represents the i th atom being added in the supercell. In this way, the root of the tree corresponds to having no H atom adsorbed on the structure, while the first level signifies having the first H atom adsorbed at a total of N possible positions. If, on the other hand, a hydrogen atom was already attached to the atom on one side of the sheet, the site on the other side belonging to the same atom is forbidden. Consequently, each node at the L th level has $(N - 2L)$ branches. Since a total of $2L$ positions have been either previously adsorbed or forbidden, this will leave $(N - 2L)$ unadsorbed sites available for adsorption on the next sequential H atom. Based on the preceding procedures, we are able to generate all the possible configurations presented in the current study. Note that some of the configurations in the data structure are identical. Therefore, by further taking the rotational and translational symmetry into account at each level, the number of distinct configurations will, in fact, be significantly less. For instance, the first level in the tree structure becomes the only branch left for further tree expansion in the graphene case, while there are two branches left in the BC_3 sheet case. The algorithm for structural comparison is similar to that used in our previous study [21]. We have implemented the aforementioned algorithm to generate all the atomic structures of H adsorptions on the 2×2 supercell. A total of 400 and 146 structural models for BC_3 and graphene, respectively, were obtained from the tree search. The computational cost to relax all these structures using first-principles calculations is relative high. Having established that a hydrogen atom tends to be on the opposite side of the sheet if the neighbor of carbon is already bonded with an H atom, this feature

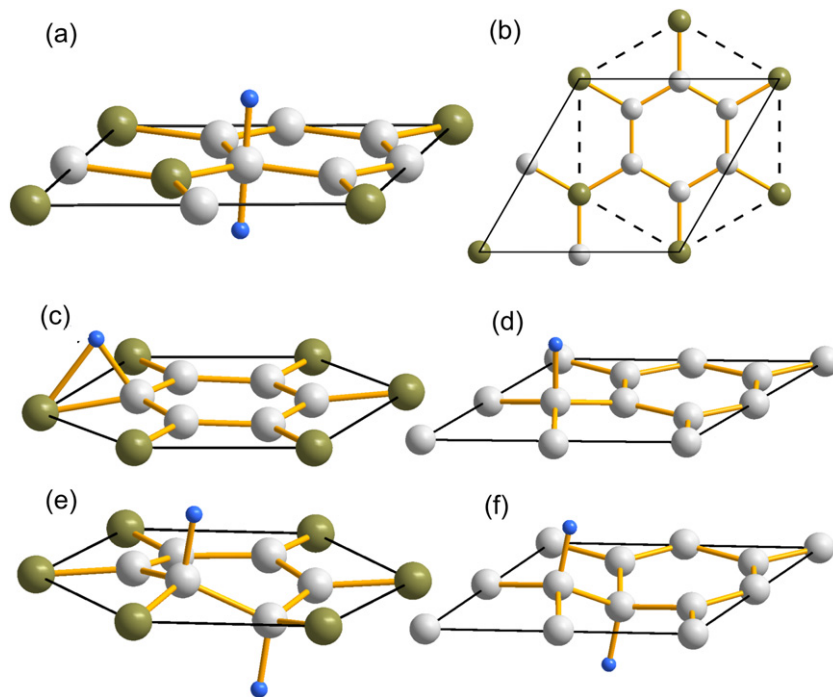


Figure 1. (a) illustrates the hydrogen can be adsorbed on both sides of the sheet. (b) shows that the supercell can be represented as a hexagon (dashed lines) or parallelogram (solid lines). (c) and (d) are the lowest energy configurations for BC₃ and graphene at H coverage of 1/8 ML. (e) and (f) are the lowest energy configurations for BC₃ and graphene at H coverage of 2/8 ML.

was further added as a constraint to the tree search. Finally, we should mention that 63 and 30 structural models for BC₃ and graphene, respectively, were obtained and then further optimized using the first-principles total energy calculations.

2.2. First-principles calculations

The calculations were carried out within the local density approximation (LDA) to density functional theory [22–24] using projector-augmented-wave potentials [25], as implemented in the Vienna *ab initio* simulation package [26]. The supercells were used to simulate the isolated sheet, and a vacuum of 10 Å was included in the supercell to reduce the interactions between sheets. We employed the 2 × 2 supercell to simulate the hydrogenation. H coverage was defined as the ratio of the number of H atoms with respect to the number of atoms in a 1 × 1 unit cell. The kinetic energy cutoff was set to 500 eV and the gamma-centered 24 × 24 × 1 Monkhorst–Pack grid was used to sample the Brillouin zone (BZ) [27]. All atoms were relaxed until the residual force on each atom was smaller than 0.001 eV Å⁻¹. For the low H coverage case, the 4 × 4 supercell and the gamma-centered 12 × 12 × 1 Monkhorst–Pack grid were used.

From the calculated total energies of the proposed models, the formation energy, ΔE_f , was computed according to the relation

$$\Delta E_f = E_n - E_{\text{clean}} - n\mu_{\text{H}}, \quad (1)$$

where E_n is the total energy of the sheet with a number of hydrogen atoms, n , adsorbed on it, E_{clean} is the energy of the sheet without any adsorption and μ_{H} is the chemical potential of H.

Alternatively, one can define the stability by looking at the formation energy per H atom which is obtained by dividing equation (1) by the number of hydrogen atoms in the supercell. Thus, the relative stabilities would not be altered by varying the chemical potential.

Lastly, the hydrogenation process can also be monitored using the adsorption energy, ΔE_{ad} , which is defined as

$$\Delta E_{\text{ad}} = E_n - E_{n-1} - \mu_{\text{H}}, \quad (2)$$

where E_{n-1} is the total energy of the sheet with $(n - 1)$ hydrogen atoms adsorbed on it.

3. Results and discussion

We have performed a systematic search for the BC₃ sheet and graphene based on the method described above. All the structures are further examined using first-principles calculations. The identified lowest energy structures for the H atom adsorbed on the 2 × 2 supercell at each coverage are illustrated in figures 1–3. The supercell can be represented either as a hexagon (dashed lines) or a parallelogram (solid lines) as shown in figure 1(b).

We first describe the hydrogenation process of the BC₃ sheet. At 1/8 ML, it turns out that the H atom prefers to be adsorbed on the carbon atom rather than on the boron atom by about 0.6 eV, residing on the C–B bond, as shown in figure 1(c). The C atom where the H atom is attached is elevated by 0.14 Å relative to the BC₃ sheet. At 2/8 ML, the lowest energy configuration is achieved when the second H atom attaches to a C atom next to another C atom where the first H atom is already

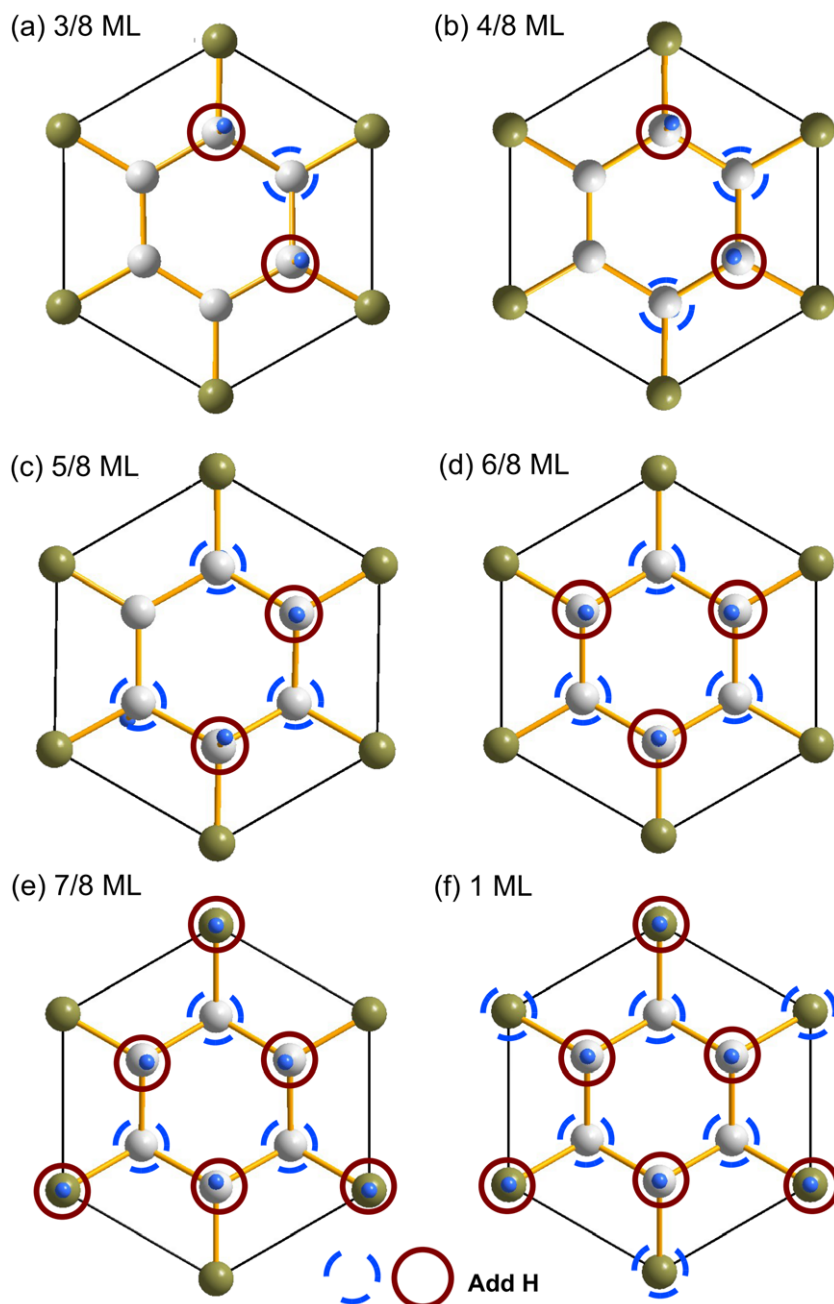


Figure 2. (a)–(f) are the top views of the lowest energy structures of H-adsorbed BC₃ sheet at hydrogen coverages ranging from 3/8 to 1 ML. Solid and dashed circles are used to indicate positions where the H atoms are adsorbed on the sheet projecting outward and inward, respectively.

attached and such that these H atoms are on opposite sides of the BC₃ sheet, as shown in figure 1(e). Here, the H atoms are only bonded to the C atoms. From 3/8 through 6/8 ML, the H atoms continue to be adsorbed on neighboring C atoms along the hexagonal ring with alternating H atoms adsorbed on either side of the BC₃. This was illustrated in figures 2(a)–(d). At 6/8 ML, every C atom is singly attached to a hydrogen atom as seen in figure 2(d). Finally at 7/8 and 8/8 ML, the hydrogen atom is bonded to the boron atoms in which the pattern whereby H is bonded on opposite sides of the sheet of the neighboring atom shown in figures 2(e) and (f) continues. We found structures with the lowest formation energy for BC₃ at 4/8 and 6/8 ML

of hydrogen are the same as those in the models proposed by Ding and Ni [18].

We now elaborate on the hydrogenation of graphene and contrast it with the corresponding hydrogenation of the BC₃ sheet. At 1/8 ML, the hydrogen can be vertically bonded to any C atom and causes this C atom to transform from an sp²-type bond back to an sp³-type bond. It differs from the BC₃ case where the H atom is above the C–B bond as shown in figure 1(c). The C–H bond length is 1.14 Å as shown in figure 1(d) and the H-adsorbed C atom is elevated by 0.28 Å from the graphene layer. At 2/8 ML, the bonding behavior is similar to that which occurred for BC₃, in which the second H

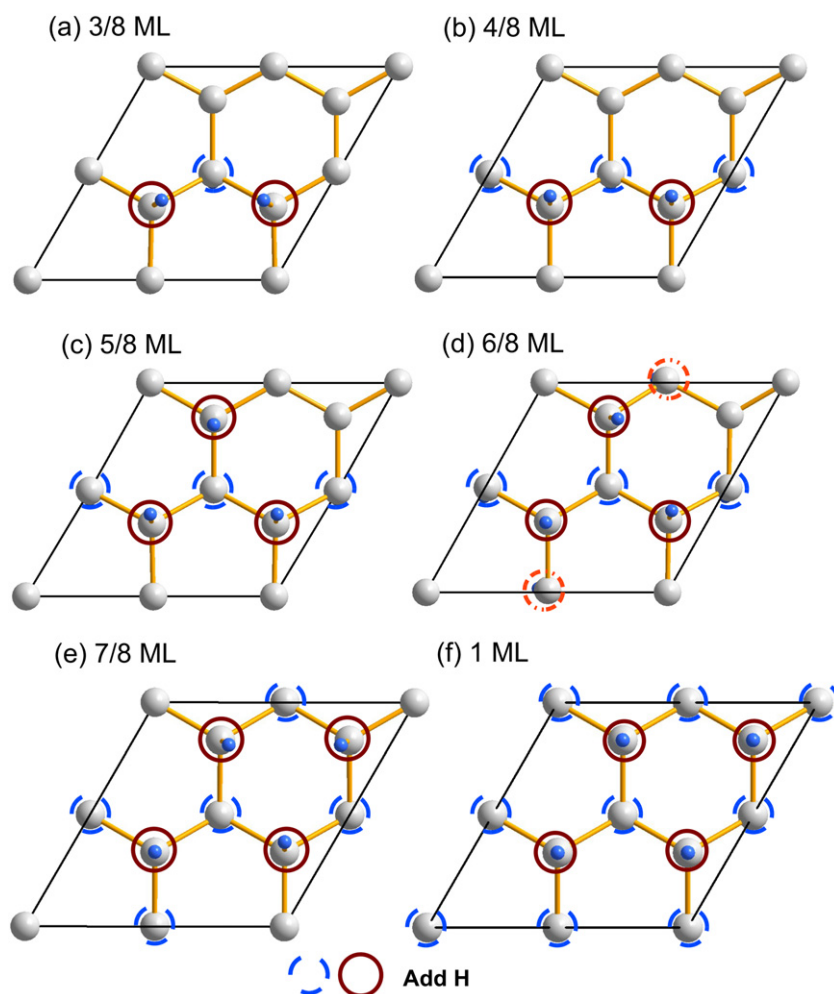


Figure 3. (a)–(f) show top views of the lowest energy structures of H-adsorbed graphene at hydrogen coverages ranging from 3/8 to 1 ML. Solid and dashed circles are used to indicate positions where the H atoms are adsorbed on the sheet projecting outward and inward, respectively.

atom is bonded to the neighboring C atom of the previous C atom on the opposite side of the sheet, as shown in figure 1(f). From 3/8 to 4/8 ML, the H atoms continue to be adsorbed on the neighboring C atoms along a certain orientation with alternating H atoms adsorbed on either side of the BC₃ as shown in figures 3(a) and (b). Likewise, from 5/8 to 8/8 ML, the H atoms are similarly adsorbed on graphene and eventually saturate all the dangling bonds as shown in figures 3(c)–(f).

To understand the mechanism of hydrogen adsorption at low coverages, we examined numerous low energy configurations for the 2 × 2 supercell and simply augmented the supercell to 4 × 4 such that a single hydrogen adsorbed on either the BC₃ sheet or graphene correspond to 1/32 ML. In addition, we manually examined various configurations for the same coverage beyond simple augmentations. We start with the H adsorption on the BC₃ sheet. In figure 4(a), the H–C bonding was found to be the same as that obtained using the 2 × 2 supercell for the BC₃. Notice that the hydrogen atom is above the B–C bond. Next, we discuss the 2/32 ML case which is obtained by adding a second H atom to the system. Here, we have tested several configurations in which two isolated H adsorptions may occur. We found that two H atoms tend

to be adsorbed on the BC₃ as illustrated in figure 4(b) which in turn is similar to that shown in figure 1(e). Adding yet another atom to the system to tackle 3/32 ML, our analysis revealed that the most stable configuration for the BC₃ sheet is the one displayed in figure 4(c). This is similar to figure 2(a). In addition, we found that a configuration consisting of a pair of H atoms adsorbed on one ring plus an isolated H atom on another ring is not preferable. Lastly, at 4/32 ML, we found that four H atoms prefer to adsorb on the same ring in the case of the BC₃ sheet.

We now discuss the case of graphene at low H coverages ranging from 1/32 to 3/32 ML. Here, we note that the lowest energy structures are identical to those using the 2 × 2 supercell. At 4/32 ML, the fourth hydrogen atoms can attach to either end of the lowest energy configuration for the 3/32 ML. Here, we note that, given any two neighboring C atoms on a graphene sheet, the H atoms should attach on opposite sides. We found two degenerate low energy configurations differing only by 12 meV per H atom as shown in figures 4(e) and (f). One appears to be a zigzag chain (figure 4(f)), while the other seems to be on the same six-membered ring which was found on graphene (see figure 4(e)). To further understand the growth

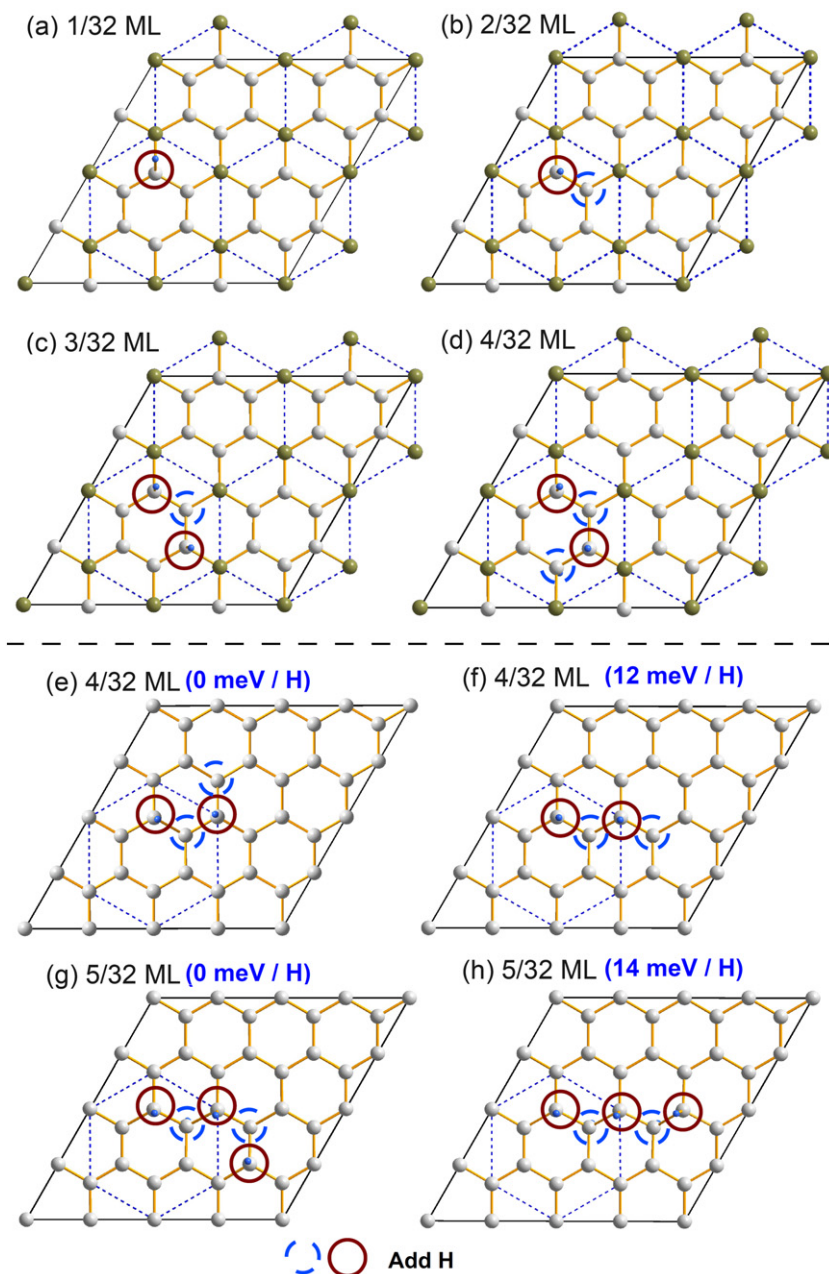


Figure 4. (a)–(d) show the top views of the lowest energy structures of H-adsorbed BC₃ at hydrogen coverages ranging from 1/32 to 4/32 ML. (e) and (f) show the lowest atomic configurations for graphene at 4/32 ML, while (g) and (h) display their counterparts at 5/32 ML. Solid and dashed circles are used to indicate positions where the H atoms are adsorbed on the sheet projecting outward and inward, respectively.

preference, we searched for the lowest energy configuration for 5/32 ML based on these two low energy configurations for 4/32 ML as shown in figures 4(e) and (f). After removing the identical structures, we found two lowest energy structures such as the ones illustrated in figures 4(g) and (h) and whose energies differ by 14 meV/H atom. The first four H atoms form a zigzag chain on graphene and the fifth H atom at either end can continue to form the zigzag chain along a certain direction. In short, it seems that the hydrogen atoms prefer to form the zigzag motif on graphene. By contrast, they were adsorbed on the same six-membered ring on the BC₃ due to the nature of the sheet structure.

To illustrate the stability due to the chemical potential, the formation energy versus the chemical potential of hydrogen is plotted in figure 5. A quick inspection of figure 5(a) reveals that for $\mu_{\text{H}} > -2.95$ eV the BC₃ sheet exhibits the greatest stability when the sheet is fully covered by H atoms. However, when $\mu_{\text{H}} < -2.95$ eV, the most stable structure is one in which only C atoms are terminated with H atoms, corresponding to an H coverage of 6/8 ML. The energy per atom of the H₂ molecule (−3.34 eV) is within this range. Similar analysis is performed on the H-adsorbed graphene and the results are illustrated in figure 5(b). Here, for $\mu_{\text{H}} > -3.98$ eV, the graphene sheet exhibits the greatest stability when the sheet

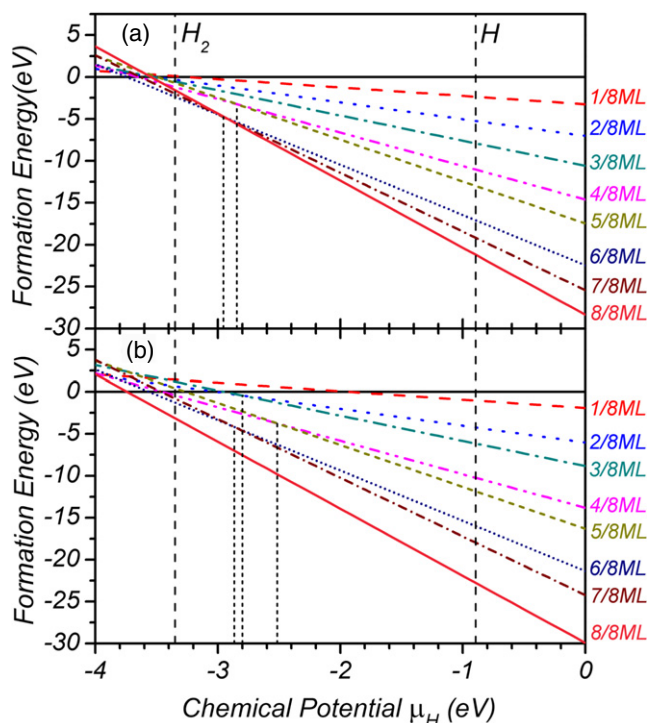


Figure 5. Formation energies of lowest energy models at different coverages versus the chemical potential for (a) BC₃ and (b) graphene.

is fully covered by H atoms. At this point, it is worth noting that an alternative way to analyze the stability is to define the formation energy per H atom obtained by dividing equation (1) by the number of hydrogen atoms in the supercell. In this way, the relative stabilities would not be altered by varying the chemical potential.

In both figures 6(a) and (b), the chemical potential is set to -3.34 eV (i.e. the total energy per atom of the H₂ molecule). The corresponding formation energies per atom coverage are plotted in figure 6(a). Figure 6(a) shows that the lowest formation energies for the BC₃ and graphene appear at 6/8 ML and 1 ML, respectively. The adsorption energy is defined as the energy difference between systems after one additional H adsorption, which is plotted in figure 6(b). It shows an even-odd oscillation of the adsorption energy, indicating that the H adsorption on the BC₃ and graphene prefer to be a pair of H atoms. It also shows that the lowest adsorption energies for BC₃ and graphene are 6/8 ML and 1 ML, respectively.

Having examined the energetics, we now turn to the electronic structure of the H-adsorbed BC₃ and graphene. The pristine BC₃ sheet itself is an indirect-gap semiconductor (ISC) with an LDA gap of 0.52 eV. For odd numbers of H atoms adsorbed on the sheet, it exhibits metallic behavior. At 2/8 ML, it is an ISC with an LDA gap of 0.54 eV. At 4/8 ML it is a direct-gap semiconductor (DSC) with a gap of 1.54 eV, while at an even higher coverage of 6/8 ML it is again a DSC, albeit with a higher gap of 1.87 eV. Finally, for 8/8 ML, it becomes a metal as shown in table 1.

In the case of graphene, we found that at the lowest coverage of 2/8 ML it is direct semiconductor (DSC) with

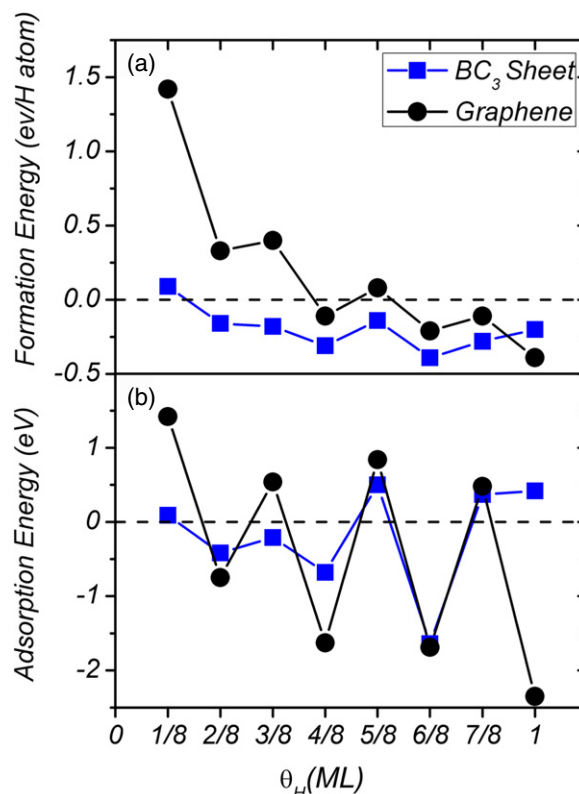


Figure 6. (a) The formation energies per H atom and (b) adsorption energies versus the H coverage for graphene and BC₃.

Table 1. The bandgaps, E_g (eV), and the properties of the H-adsorbed BC₃ sheet and graphene versus the coverage of H, θ_H (ML). They behave as either metal (M), indirect semiconductor (ISC) or direct semiconductor (DSC).

θ_H	BC ₃		Graphene		
	LDA	GGA	LDA	GGA	
0/8	0.52	(0.76) ^a	ISC	0.00	DSC
1/8	0.00		M	0.00	M
2/8	0.54		ISC	0.00	DSC
3/8	0.00		M	0.00	M
4/8	1.54		ISC	0.00	M
5/8	0.00		M	0.00	M
6/8	1.87	(2.11) ^a	DSC	3.41	DSC
7/8	0.00		M	0.00	M
1	0.00	(0.00) ^a	M	3.43	(3.50) ^b DSC

^a Reference [18]. ^b Reference [5].

a zero bandgap, similar to the pure graphene sheet. At H coverages of 6/8 and 1 ML, H-adsorbed graphene exhibits direct bandgaps of 3.41 eV and 3.43 eV, respectively. For the rest of the coverages considered, the H-adsorbed graphene is metallic. It is noted that, for BC₃ and graphene with an odd number of H atoms, the system demonstrates metallic properties. Additionally, we also found that at 1 ML, graphene exhibits semiconducting behavior with a large bandgap due to the sp³ hybridization [4, 19]. In the case of BC₃ materials with either 6/8 or 1 ML, its dominant electronic properties are ascribed to the bonding status of the boron p_z orbitals [18].

Table 2. The calculated work functions, ϕ , of the hydrogen-adsorbed sheets versus the hydrogen coverage. For even numbers of H atoms per 2×2 supercell, the numbers of H atoms on either side are equal, while for the odd number of H atoms the number of H atoms on one side is greater than that on the other side. We denote the work function of the side with more adsorbed H atoms as $\phi_>$, and that with less adsorbed H atoms as $\phi_<$.

θ_{H} (ML)	BC ₃		Graphene			
	$\phi_<$	ϕ	$\phi_>$	$\phi_<$	ϕ	$\phi_>$
0/8		5.73			4.49	
1/8	5.40		4.66	4.58		3.72
2/8		5.01			4.16	
3/8	4.91		4.28	4.05		3.58
4/8		4.49			3.79	
5/8	4.12		3.72	3.48		3.13
6/8		4.01			5.19	
7/8	4.77		5.32	3.36		3.34
1		5.66			4.90	

We further calculated and summarized the work functions of the hydrogen-adsorbed BC₃ sheet and graphene at various H coverages in table 2. The method used in calculating the work function can also be found in [28]. For the coverages in which the H-adsorbed sheets show semiconducting properties, the Fermi level was set to the highest occupied molecular orbital states instead of the middle of the bandgap. The work functions for the pure BC₃ sheet and graphene are calculated to be 5.73 and 4.49 eV, respectively. We found that generally the hydrogen-adsorbed BC₃ sheet and graphene have a lower work function than the pure BC₃ sheet and graphene, except for the hydrogen-adsorbed graphene at 1/8, 6/8 and 1 ML. As the hydrogens were adsorbed onto either the BC₃ sheet or graphene, the corresponding work function values are altered by different coverages of H, as seen in table 2. The resulting lower work function at low coverage can be attributed to the presence of small dipoles on C–H bonds [29], C^{σ⁻}–H^{σ⁺}, owing to the stronger electronegativity of C. Such an effect would give a qualitative understanding of the modified work function due to the effects of hydrogen adsorption. For graphene, the side with fewer H atoms seems to have a higher value of the work function. This trend is replicated in the case of the BC₃ sheet when the H coverage is less than 6/8 ML. At 7/8 ML, the H atoms start to be adsorbed on the B atoms and the work function of the side with fewer H atoms instead has a lower value than the other side.

4. Conclusions

We have performed a comparative study of the hydrogenated BC₃ sheet and graphene using first-principles calculation. For the BC₃ sheet, our calculations show that hydrogen atoms prefer to be adsorbed on C rather than B. For both the hydrogen-adsorbed BC₃ sheet and graphene, the most stable configurations are those with H coverages of 6/8 ML and 1 ML, respectively. The preferred hydrogen arrangement on the single BC₃ layer is similar to that on graphene where the adsorbed H atoms on the neighboring C atoms are on the opposite sides of the sheet. Moreover, at low

coverage of H, the pattern of the hydrogen adsorptions on the BC₃ shows a preference towards forming on the same ring, whereas on graphene the zigzag chain is more likely. Lastly, the hydrogenated BC₃ sheet and graphene exhibit alternation of semiconducting and metallic properties as the H concentration is increased. These results suggest the possibility of manipulating the bandgaps in the single BC₃ sheet and graphene by varying the H concentrations.

Acknowledgments

The authors acknowledge support from the National Center for Theoretical Sciences (NCTS) and the National Science Council (NSC) of Taiwan under grant nos. NSC-98-2112-M110-002-MY3 (FCC) and NSC-99-2112-M-492-001-MY2 (WSS). We are grateful to the National Center for High-performance Computing (NCHC) for computer time and facilities.

References

- [1] Stankovich S, Dikin D A, Dommett G H B, Kohlhaas K M, Zimney E J, Stach E A, Piner R D, Nguyen S T and Ruoff R S 2006 *Nature* **442** 282
- [2] Berger C *et al* 2006 *Science* **312** 1191
- [3] Yang C K 2009 *Appl. Phys. Lett.* **94** 163115
- [4] Sofo J O, Chaudhari A S and Barber G D 2007 *Phys. Rev. B* **75** 153401
- [5] Boukhalov D W, Katsnelson M I and Lichtenstein A I 2008 *Phys. Rev. B* **77** 035427
- [6] Son Y-W, Cohen M L and Louie S G 2006 *Phys. Rev. Lett.* **97** 216803
- [7] Li X L, Wang X R, Zhang L, Lee S W and Dai H J 2008 *Science* **319** 1229
- [8] Ritter K A and Lyding J W 2009 *Nat. Mater.* **8** 235
- [9] Son Y-W, Cohen M L and Louie S G 2006 *Nature* **444** 347
- [10] Ryu S, Han M Y, Maultzsch J, Heinz T F, Kim P, Steigerwald M L and Brus L E 2008 *Nano Lett.* **8** 4597
- [11] Elias D C, Nair R R, Mohiuddin T M G, Morozov S V, Blake P, Halsall M P, Ferrari A C, Boukhalov D W, Katsnelson M I and Geim A K 2009 *Science* **323** 610
- [12] Tanaka H, Kawamata Y, Simizua H, Fujitaa T, Yanagisawaa H, Otanic S and Oshima C 2005 *Solid State Commun.* **136** 22
- [13] Yanagisawa H, Tanaka T, Ishida Y, Rokuta E, Otani S and Oshima C 2006 *Phys. Rev. B* **73** 045412
- [14] Tomanek D, Wentzcovitch R M, Louie S G and Cohen M L 1988 *Phys. Rev. B* **37** 3134
- [15] Wang Q, Chen L Q and Annett J F 1996 *Phys. Rev. B* **54** R2271
- [16] Pontes R B, Fazzio A and Dalpian G M 2009 *Phys. Rev. B* **79** 033412
- [17] Ding Y, Wang Y and Ni J 2009 *Appl. Phys. Lett.* **94** 073111
- [18] Ding Y and Ni J 2009 *J. Phys. Chem. C* **113** 18468
- [19] Lebègue S, Klintonberg M, Eriksson O and Katsnelson M I 2009 *Phys. Rev. B* **79** 245117
- [20] Cormen T H, Leiserson C E, Rivest R L and Stein C 2001 *Introduction to Algorithms* 2nd edn (Cambridge, MA: MIT Press)
- [21] Wu B-R, Huang Z-Q, Su W-S, Hsieh Y-Y and Chuang F-C 2010 *Diamond Relat. Mater.* **19** 1341
- [22] Hohenberg P and Kohn W 1964 *Phys. Rev.* **136** B864
Kohn W and Sham L J 1965 *Phys. Rev.* **140** A1135

- [23] Ceperley D M and Alder B J 1980 *Phys. Rev. Lett.* **45** 566
- [24] Perdew J P and Zunger A 1981 *Phys. Rev. B* **23** 5048
- [25] Kresse G and Joubert D 1999 *Phys. Rev. B* **59** 1758
- [26] Kresse G and Hafner J 1993 *Phys. Rev. B* **47** 558
Kresse G and Furthmuller J 1996 *Phys. Rev. B* **54** 11169
- [27] Monkhorst H J and Pack J D 1976 *Phys. Rev. B* **13** 5188
- [28] Leung T C, Kao C L, Su W S, Feng Y J and Chan C T 2003
Phys. Rev. B **68** 195408
- [29] Su W S, Leung T C, Li B and Chan C T 2007 *Appl. Phys. Lett.*
90 163103